

Electrocatalytic Evolution of Oxygen Gas at Cobalt Oxide Nanoparticles Modified Electrodes

*Ibrahim M. Sadiq, Ahmad M. Mohammad, Mohamed E. El-Shakre, M. Ismail Awad, Mohamed S. El-Deab, and Bahgat E. El-Anadouli**

Chemistry Department, Faculty of Science, Cairo University, P.O. 12613 – Giza, Egypt

*E-mail: bahgat30@yahoo.com

Received: 19 December 2011 / *Accepted:* 27 February 2012 / *Published:* 1 April 2012

The electrocatalysis of oxygen evolution reaction (OER) at cobalt oxide nanoparticles (nano-CoO_x) modified GC, Au and Pt electrodes has been examined using cyclic voltammetry. The OER is significantly enhanced upon modification of the electrodes with nano-CoO_x, as demonstrated by a negative shift in the polarization curves at the nano-CoO_x modified electrodes compared to that obtained at the unmodified ones. Scanning electron microscopy (SEM) revealed the electrodeposition of nanometer-size CoO_x (average particle size of 200 nm) onto GC electrode. Optimization of the operating experimental conditions (i.e., solution pH and loading level of nano-CoO_x) has been achieved to maximize the electrocatalytic activity of nano-CoO_x modified electrodes. It has been found that the electrocatalytic activity of the nano-CoO_x modified electrodes towards the OER is pH and loading level dependent, while it is substrate independent. The low cost as well as the marked stability of the thus-modified electrodes make them promising candidates in industrial water electrolysis process.

Keywords: Nanostructures; Water electrolysis; Cobalt oxide; Electrocatalysis

1. INTRODUCTION

The oxygen evolution reaction (OER) attracts a reasonable deal of attention as a consequence of its importance in a wide range of industrial applications such as water electrolysis, energy conversion and storage devices. Metal oxide-based anodes, particularly those of nickel and cobalt, have long been used to catalyze the OER in alkaline electrolyzers due to their remarkable stability and activity [1-11]. Of these oxides, the spinel Co₃O₄ oxide exhibited the highest catalytic efficiency and stability towards the OER in alkaline medium [6]. This spinel Co₃O₄ oxide can unlikely be prepared in

a single pure phase. Instead, several other oxide CoO_x phases are always accompanying it in the form of mixed oxide phases.

It is important to recognize that the electrocatalytic activity for OER on metal oxides whose metals exist in the highest oxidation state and no further oxidation is possible (*e.g.*, NiO_2 and CoO_2), is always low. These observations seem to agree with the suggestions proposed by Tseung and Jasem [12] and Trasatti [13, 14] that the lower/higher couples of oxidation states are required for the OER. Also, the influence of the oxide film conductivity is important and most likely depends on the oxide phase itself and the film thickness.

The interest in the OER has significantly enlarged with the advanced revolution in nanotechnology. In this context, various nanoparticle-based modified anodes were suggested to catalyze this reaction [15, 16]. Nanoparticle-modified electrodes show a unique catalytic enhancement due to the significant increase in the surface area to volume ratio (geometric factor) and/or the improvement in the electronic properties. In this regard, tailoring the regular electrode materials with nanostructures of transition metal/oxides resulted in an interesting electrocatalytic enhancement towards the OER by orders of magnitude compared to that obtained at the bare electrodes [15-18]. Herein, three different conventional electrodes (Au, Pt and GC) are going to be modified with cobalt oxide nanoparticles (nano- CoO_x) for the sake of enhancing their electrocatalytic activity towards the OER. Their electrocatalytic activity was optimized via investigating the effect of pH and the loading extent of the nano- CoO_x .

2. EXPERIMENTAL

Glassy carbon (GC, $d = 3.0$ mm), polycrystalline gold, poly-Au ($\varphi = 1.6$ mm), and polycrystalline platinum, poly-Pt ($\varphi = 1.6$ mm) were used as working electrodes. A Ag/AgCl/KCl (sat.) and a spiral Pt wire were served as the reference and counter electrodes, respectively. Conventional pretreatment methods were applied to clean the GC, Au and Pt electrodes. Typically, the electrodes were mechanically polished with aqueous slurries of fine alumina powder. Moreover, the Au and Pt electrodes were electrochemically pretreated in 0.5 M H_2SO_4 solution by cycling the potential until obtaining a typical characteristic cyclic voltammogram (CV) for clean poly-Au and poly-Pt electrodes (cf Fig. 1C curve a as an example for a clean poly-Au electrode).

The fabrication of the nano- CoO_x on the electrode surface was carried out by the cyclic voltammetry technique. Typically, the potential was scanned for 15 potential cycles with a scan rate of 100 mVs^{-1} in the potential range between 1.2 V and -1.1 V vs. Ag/AgCl/KCl (sat.) in phosphate buffer solution (PBS, (pH = 7.0) containing 1mM $\text{CoCl}_2 \cdot 6\text{H}_2\text{O}$).

A Field Emission Scanning Electron Microscope, FE-SEM (FEI, QUANTA FEG 250) attached with energy dispersive X-ray spectrometer (EDS) was used to evaluate the electrode morphology and to distinguish the different composition on the electrode surface.

All chemicals used in this investigation were of analytical grades and were used without further purification. All electrochemical measurements were performed at room temperature ($25 \pm 1^\circ\text{C}$) using a

computer-controlled EG&G 273A potentiostat. All current densities were calculated on the basis of the geometric surface area of the relevant working electrodes.

3. RESULTS AND DISCUSSION

3.1. Characterization of nano-CoO_x modified electrodes

Fig. 1(A) shows the FE-SEM images of the GC substrate, at two different magnifications, after the modification with electrodeposited cobalt oxide. This figure depicts the formation of some nanometer-scale agglomerates of CoO_x. The formation of such fused nanoparticles may be attributed to the high rate of particle growth over nucleation rate of new particles.

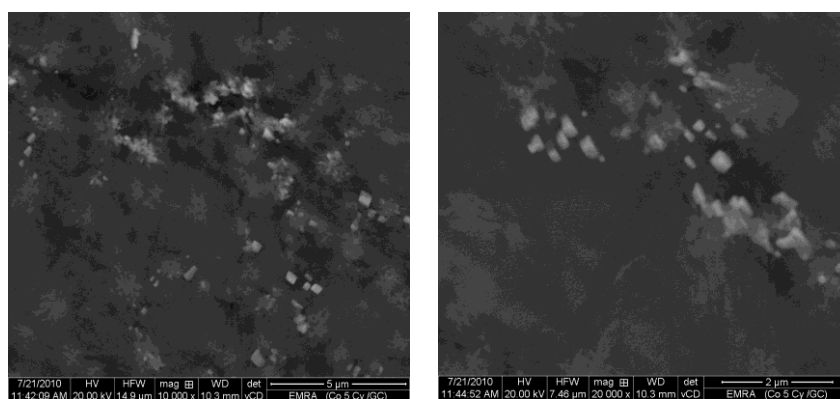


Figure 1.(A) FE-SEM micrographs of the electrodeposited CoO_x on the GC substrate. Note that CoO_x is electrodeposited as described in the experimental section.

The electrochemical characterization of the electrodeposited nano-CoO_x on GC electrode surface was carried out by measuring the CVs of the unmodified and nano-CoO_x modified GC (nano-CoO_x/GC) electrodes in 0.5 M KOH solution (Fig. 1(B)). This figure shows two oxidation peaks (I_a) and (II_a) at the modified electrode during the positive-going potential scan, Namely, at 160 mV and 530 mV, respectively. The corresponding two reduction peaks (I_c and II_c) during the negative-going potential scan appears at 80 mV and 480 mV, respectively. These two redox couples are assigned to the conversion between the different phases of cobalt oxides [19-22].

Fig. 1(C) shows the characteristic CV of the unmodified and nano-CoO_x modified Au (nano-CoO_x/Au) electrodes measured in air –saturated 0.5 M H₂SO₄. A typical CV characteristic for poly-Au electrode is shown as a solid curve. That is the oxide formation commences at a potential 1.1 V, which extends up to 1.5 V, during the anodic-going potential scan. On the other hand, the reduction of Au-oxide is observed as a reduction peak centered at ca. 0.9 V. The slight decrease in the intensity of the reduction peak of the Au-oxide monolayer (at ca. 0.9 V, shown for unmodified Au, solid curve) with the modification with CoO_x (dashed curve) indicates the effective deposition of CoO_x at the Au

electrode surface. Utilizing this observation, The real surface areas of the unmodified (A_{bare}) and nano-CoO_x modified (A_{mod}) Pt and Au electrodes were estimated based on the charge associated with the reduction of the Au and Pt oxide layers, respectively, utilizing a reported value of 420 and 400C/cm² [23, 24], respectively and consequently, the surface coverage (θ) of nano-CoO_x can be estimated using the following equation;

$$\theta = 1 - \left(\frac{A_{mod}}{A_{bare}}\right) \tag{1}$$

where A_{bare} and A_{mod} are the real surface area of the unmodified and nano-CoO_x modified electrodes, respectively.

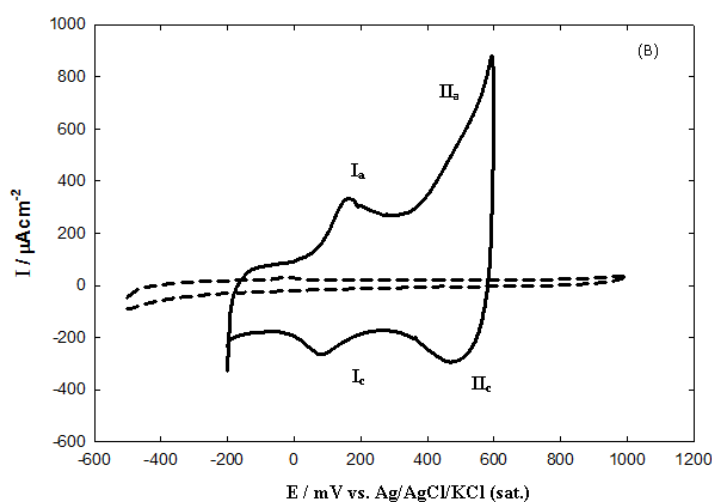


Figure 1. (B) CV response of the bare (dashed curve) and nano-CoO_x/GC (solid curve) electrodes in 0.5 M KOH. Note that CoO_x is electrodeposited as described in the caption of Fig. 1A.

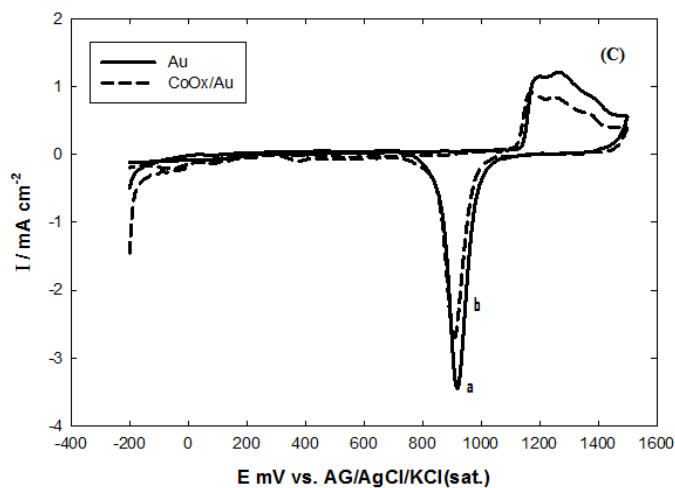


Figure 1. (C) CV response obtained in 0.5 M H₂SO₄ at nano-CoO_x/Au (dashed curve) and bare Au electrodes (solid curve).

3.2. The OER at nano-CoO_x modified electrodes

The electrocatalytic activity of the nano-CoO_x modified GC, Au and Pt electrodes was investigated by measuring the linear sweep voltammetry (LSV) in 0.5 M KOH which are shown in Fig. 2 (A-C). This figure reveals a significant enhancement in the electrocatalytic activity towards the OER upon the modification of Au, Pt and GC with nano-CoO_x. The onset potentials of the OER at the nano-CoO_x modified GC, Au, and Pt electrodes are shifted towards the negative direction. As depicted from Fig. 2, the OER commences at the same potential (with onset potential of ca. 600 mV) at the three modified electrodes (i.e., the electrocatalytic enhancement of the nano-CoO_x modified GC, Au and Pt electrodes towards the OER is substrate independent). In addition, the calculated polarization slopes of both unmodified and nano-CoO_x modified GC, Au and Pt electrodes are found to be parallel with a slope close to 120 mV/decade.

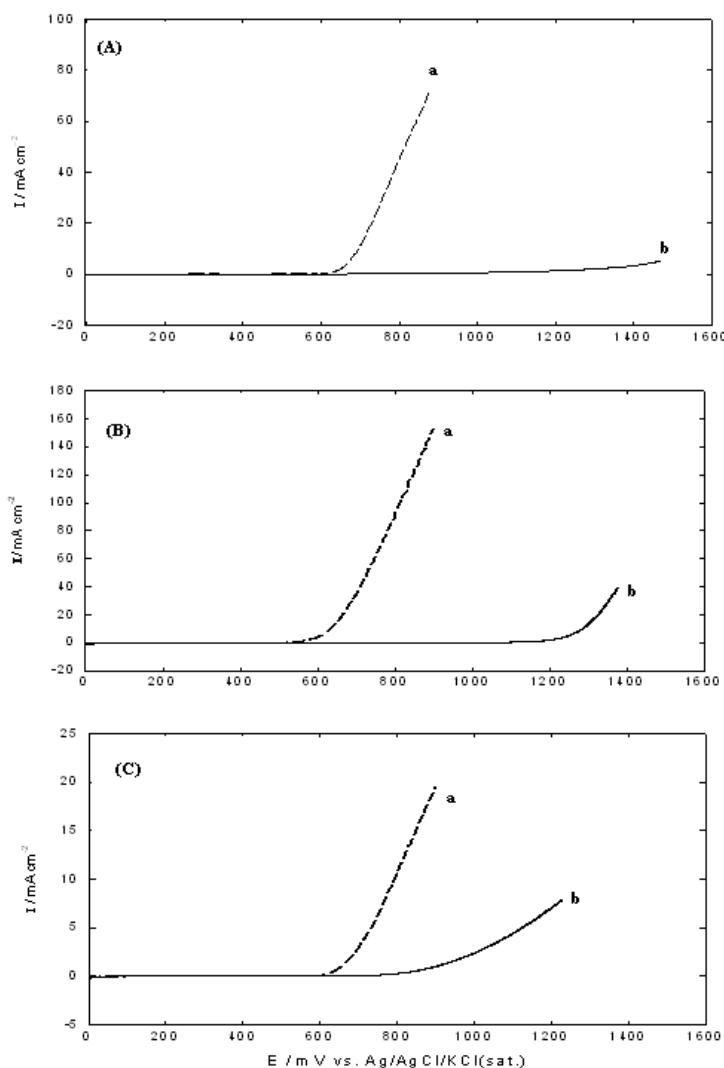


Figure 2. (A-C) LSV response for the OER in 0.5 M KOH at the unmodified (curve b) and the nano-CoO_x (curve a) modified (A) GC, (B) Au and (C) Pt electrodes at potential scan rate of 20 mV s⁻¹.

The similarity of the polarization slopes indicates that oxygen evolution proceeds via a common rate-determining step in both cases. The Tafel slopes of ca. 120 mV/decade ($b = 2.303RT/anF$, α : the anodic transfer coefficient) indicate that the water discharge is the rate-determining step. Which is consistency with a recently published data for the OER at GC, Au, and Pt electrodes modified with nickel oxide nanoparticles (nano-NiO_x) [16]. This means that modifying any relatively cheap substrate, albeit with a good resistance against corrosion, with the cheap nano-CoO_x would represent a promising anode in water electrolysis. It is worth mentioning here that, the substrate independent behavior towards the OER observed in the current study is opposite to that observed in case of the OER at manganese oxide nanorods modified electrodes [15]. In this earlier report, the maximum enhancement was obtained at the MnO_x-nanorods modified Au electrode (expensive material), whereas, a relatively lower enhancement has been obtained at the MnO_x-nanorods modified GC electrode.

It is commonly acceptable [25] to express potential in terms of the oxygen overpotential, η , i.e.,

$$\eta = E_{\text{irr}} - E_{\text{rev}} \quad (2)$$

where, E_{irr} is the irreversible electrode potential (the measured electrode potential, E_{meas}) and E_{rev} is the reversible electrode potential. For the OER ($E_{\text{rev}} = 1.23 - 0.059 \text{ pH}$) vs. SHE, at pH 14 (0.5 M KOH) $E_{\text{rev}} = 0.404 \text{ V}$ vs. SHE. When the reference electrode is Ag/AgCl electrode in the same solution as the working anode $E_{\text{rev}} = 0.207 \text{ V}$. Clearly, in this case η is related to the voltage, E_{meas} , measured on the Ag/AgCl scale as follows:

$$\eta = E_{\text{meas}} - 0.207 \text{ V} \quad (3)$$

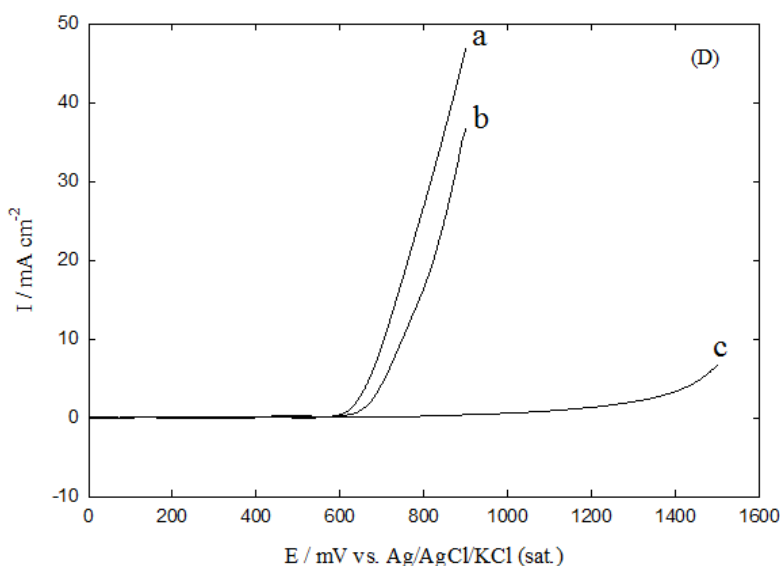
Table 1 lists the oxygen evolution overpotentials (η) at the nano-CoO_x modified GC, Au, and Pt electrodes in 0.5 M KOH at various current densities. There is a slight variation of the values of η at the three substrates, at the same current density, which might be attributed to variations in the loading level of the electrodeposited nano-CoO_x at the different electrodes, albeit using the same experimental conditions.

This urged us to study the effect of loading level of nano-CoO_x (cf. Section 3.4). The values of η at the nano-CoO_x (listed in Table 1) are comparable to those obtained at the nano-MnO_x [15] and nano-NiO_x [16] modified electrodes. Interestingly, these values are lower than the reported values in the literature for the spinel [26, 27] and perovskite-types [28] at the same current densities.

Fig. 2 (D) shows the LSV response for the OER at the nano-CoO_x (curve a), and the nano-NiO_x (curve b) modified GC electrodes. This figure shows how better the enhancement in the electrocatalytic activity of the OER is on the nano-CoO_x modified electrodes relative to that of the nano-NiO_x modified GC electrodes. That is, the current density of the OER (i.e., rate of OER) at the optimum loading of nano-CoO_x modified electrodes is less positive by 80 mV than the current density of the OER at the optimum loading nano-NiO_x modified GC electrodes.

Table 1. Oxygen evolution overpotential at nano-CoO_x modified GC, Au and Pt electrodes in 0.5 M KOH at different current densities.

$I / \text{mA cm}^{-2}$	$\frac{\eta_{\text{O}_2} / \text{mV}}{\text{CoO}_x/\text{GC}}$	CoO _x /Au	CoO _x /Pt
5	456	423	459
10	483	453	567
15	500	468	580
20	517	487	610
25	530	496	643
30	542	506	677

**Figure 2. (D)** LSV response for the OER obtained in 0.5 M KOH at (a) nano-CoO_x/GC, (b) nano-NiO_x/GC electrodes, and (c) bare GC electrode at potential scan rate of 20 mV s⁻¹.

3.3 Effect of pH

The effect of solution pH on the electrocatalytic activity of the nano-CoO_x modified electrodes towards the OER was examined by measuring the LSVs at the unmodified and the nano-CoO_x modified GC, Au, and Pt electrodes at various pH values (data are not shown). The cathodic potential shift at a current density of 10 mA cm⁻² (ΔE_{10}) is presented in Table 2. As depicted from this table, the maximum ΔE_{10} of the OER was obtained in alkaline solution (pH > 7); similar to a previous observation at the nano-NiO_x modified electrodes [16]. On the other hand, in acidic and neutral solution (pH ≤ 7), a significantly decrease of the electrocatalytic activity is observed at the modified Au and Pt electrodes and a slight decrease of the electrocatalytic activity is observed at the modified GC electrode, presumably due to the low stability of the active phase of CoO_x. Because under these conditions of pH and potential cobalt present in the form of Co²⁺ which is responsible for the observable decrease in the electrocatalytic activity at neutral and acidic media [29].

Table 2. Variation of ΔE_{10} of the OER obtained at nano-CoO_x modified GC, Au and Pt electrodes with pH of the solution.

pH	$\Delta E_{10} / \text{mV}$		
	CoO _x /GC	CoO _x /Au	CoO _x /Pt
14	815	655	505
11	385	560	225
9	365	510	225
7	105	380	95
4	100	10	10
2	100	10	10

3.4. Effect of the loading level

The effect of loading of the nano-CoO_x on the electrocatalytic activity towards the OER is investigated to achieve the highest catalytic activity. As mentioned in Section 2, CoO_x was electrodeposited by a potential cycling method, the number of potential cycles was varied to control the loading level of the nano-CoO_x on the different electrodes. The corresponding LSVs of the OER at nano-CoO_x modified GC electrodes were recorded in 0.5 M KOH and shown in Fig. 3.

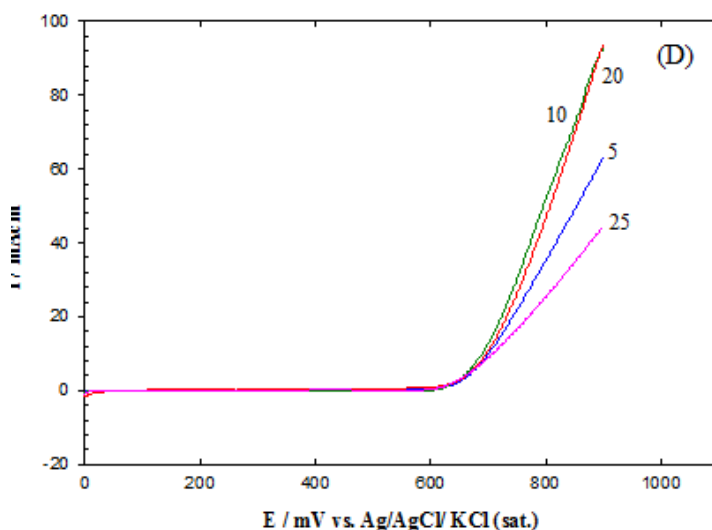


Figure 3. LSV response for the OER in 0.5M KOH at nano-CoO_x/ GC electrode prepared by different potential cycles (5, 10, 20 and 25 pot. cycles) at a potential scan rate of 20 mV s⁻¹. The numbers refer to the potential cycles employed for the deposition of nano-CoO_x.

Two interesting points can be evaluated upon inspecting Fig. 3:

(i) Insignificant change of the onset potential of the OER at the nano-CoO_x GC electrode with various loadings of nano-CoO_x. This can be explained on the basis that the onset potential of the OER is an intensive property, *i.e.*, it is independent of the amount of the nano-CoO_x. This behavior agrees with the results obtained at nano-MnO_x modified Au electrode [30].

(ii) The catalytic enhancement of the OER increases at the beginning with the increase in the number of potential cycles (*i.e.*, the extent of loading of nano-CoO_x). The highest negative shift was obtained at the GC electrode after depositing the nano-CoO_x for 10 potential cycles. When the number of potential cycles increased to 25, a significant reduction the electrocatalytic activity was noticed (the polarization curves shifted to lower currents).

Similar results were obtained at nano-CoO_x modified Au and Pt electrodes (Data are not shown), where the enhancement increases with increasing the number of cycles employed for the CoO_x deposition till a certain loading after which an adverse effect is observed.

3.5. The effect of ageing

The effect of ageing on the electrocatalytic activity of the modified electrodes was examined by cycling the potential several times between -200 mV to 600 mV on the nano-CoO_x modified GC electrode in 0.5 M KOH and recording the corresponding LSV in the same solution. Fig. 4 shows the CVs of the nano-CoO_x modified GC electrode in 0.5 M KOH after ageing for 100, 300, and 500 potential scans. Interestingly, a stable redox behavior with almost similar peak currents was obtained (Fig. 4) indicating the high stability of CoO_x at the prevailing operating conditions of pH and potential window. The corresponding LSVs for the OER at the same electrode are shown in Fig. 5. The onset potential for the OER remained the same but the kinetics got slightly slower (*i.e.*, currents shifts to lower values) with the number of aging cycles. Nevertheless, the stability of the nano-CoO_x modified electrodes is much better than that obtained at the nano-NiO_x modified electrodes upon treating similarly [16].

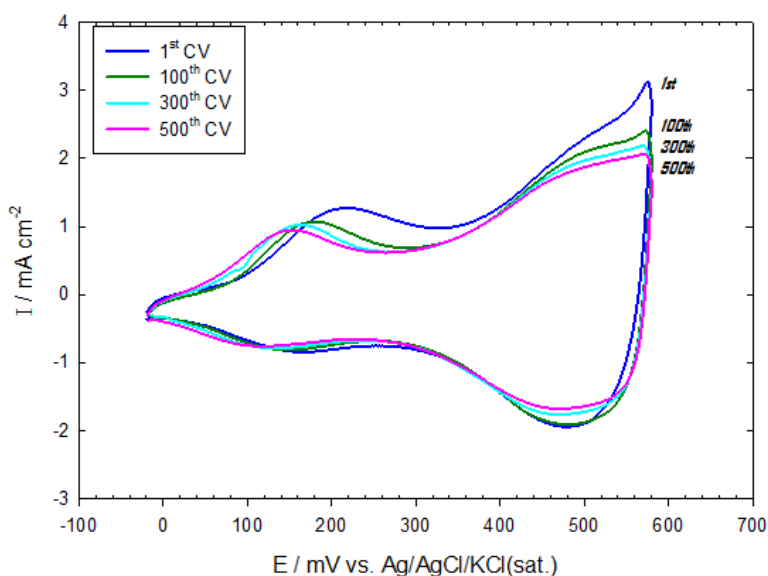


Figure 4. CV responses at the nano-CoO_x/GC electrode in 0.5 M KOH after ageing for several potential cycles (1st, 100, 300 and 500 potential cycles).

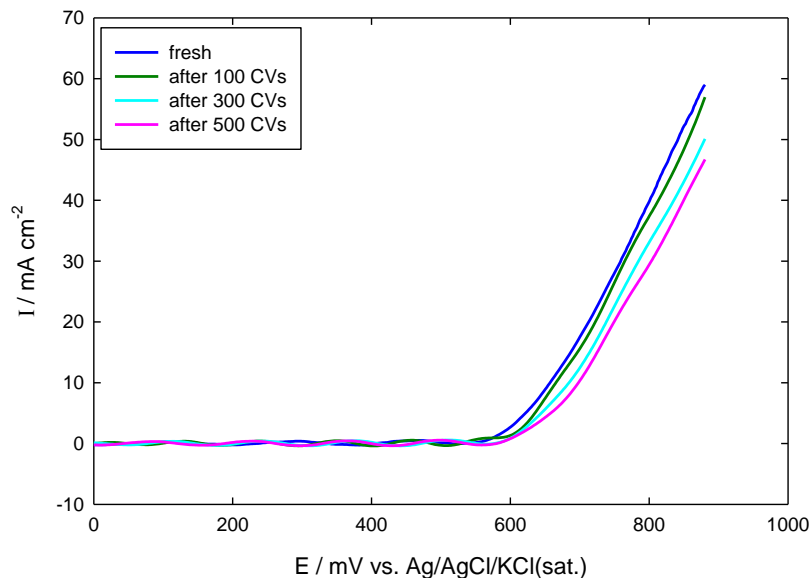


Figure 5. The LSV response of the OER in 0.5 M KOH at the nano-CoO_x/GC after ageing in 0.5 M KOH for several potential cycles up to 500 CVs (see **Fig. 4**).

3.6. Energy savings

The values of the rate of power savings per gram of oxygen gas were calculated and listed in table 3. The significant decrease in the potential obtained after the modification with nano-CoO_x corresponds to a reduction in the rate of energy consumption at the anode and consequently, decreases the energy consumption in the overall process. The energy saving in watt hours, $\Delta W_{(a)}$ at the anode at a particular current, i , is given by:

$$\Delta W_{(a)} = \left(\frac{i \Delta E_{(a)} t}{3600} \right) \tag{3}$$

where t is the electrolysis time in seconds, $\Delta E_{(a)}$ is the cathodic shift in the potential at a particular current at the anode after the modification with nano-CoO_x. The values of $\Delta E_{(a)}$ were obtained from Fig. 2 (A-C). The amount of oxygen gas produced (in g equiv.) is given by Faraday's law as (it/F) . Consequently, the energy saving, P , at the anode per gram of oxygen gas is given by:

$$P_{(a)} = \frac{i \Delta E_{(a)} (t/3600)}{i(t/F)} = \frac{\Delta E_{(a)} F}{3600} \tag{4}$$

where P is the W h per gram of oxygen gas. The value of P calculated at different current densities and listed in table 3. From the data in table 3, the best energy saving per gram of oxygen gas is obtained at nano-CoO_x modified GC electrode. The values of energy saving per gram of oxygen gas at the nano-CoO_x modified GC electrode decreases with the increase in current density which can be attributed to the effect of bubbles on the ohmic drop and on the stability of the film. The values of

energy saving per gram of oxygen gas at the nano-CoO_x modified Au electrode is mainly the same which may be attributed to the greater the calculated exchange current density (i_0 /A cm⁻²) for the OER at Au substrate [16].

Table 3. The cathodic shift in the potential and the rate of energy saving (W h g⁻¹) at the anode obtained after the modification with nano-CoO_x at various current densities

I / (mA cm ⁻²)	$\Delta E_{(c)}$ / mV			P / kW h kg ⁻¹		
	GC	Au	Pt	GC	Au	Pt
5	840	650	390	22.5	17.4	10.4
10	810	650	440	21.7	17.4	11.7
20	770	640	319	20.6	17.1	8.50
30	750	660	...	20.1	17.6	...
40	720	660	...	19.3	17.6	...

4.CONCLUSIONS

Cheap, efficient, and stable nano-CoO_x-based anodes fabricated by potential cycling method which resulted in deposition of CoO_x in the form nanometer-scale aggregates are proposed as electrocatalysts for the OER. The maximum electrocatalytic activity towards the OER was obtained in alkaline media (pH > 9). The electrocatalytic activity is independent of the nature of the substrate. The electrocatalytic activity of the modified electrodes increased with the number of potential cycles employed for the CoO_x deposition till a certain loading beyond which an adverse effect is observed. A stable redox behavior with almost similar peak currents was obtained after cycling the potential for 500 times indicating the high stability of CoO_x at the prevailing operating conditions of pH and potential window. The thus-fabricated nano-CoO_x modified electrodes exhibited a good stability and durability as revealed from the aging experiments. The values of energy saving per gram of oxygen gas at a current density of 10 mA cm⁻² GC, Au, and Pt electrodes are 22.5, 17.4, and 10.4 kW h kg⁻¹, respectively.

ACKNOWLEDGEMENT

I. M. Sadiq thanks the Graduate Research Challenge Fund (GRCF) from Cairo University during his M.Sc. research project (No. 0106030007).

References

1. A. K. M. Fazle Kibria, S. A. Tarafdar, *Int. J. Hydrogen Energy*, 27 (2002) 879.
2. M. E. G Lyons, M. Brandon, *Int. J. Electrochem. Sci.*, 3 (2008) 1386.
3. M. E. G. Lyons, M. P. Brandon, *J. Electroanal. Chem.*, 641(2010) 119.
4. Y. Zhang, X. Cao, H. Yuan, W. Zhang, Z. Zhou, *Int. J. Hydrogen Energy*, 24 (1999) 529.
5. C. Bocca, G. Cerisola, E. Magnone, A. Barbucci, *Int. J. Hydrogen Energy*, 24 (1999) 699.

6. M. Hamdani, R.N. Singh, P. Chartier, *Int. J. Electrochem. Sci.*, 5 (2010) 556.
7. M. E. G. Lyons, M. P. Brandon, *Int. J. Electrochem. Sci.*, 3 (2008)1425
8. E. Laouini, M. Hamdani, M. I. S. Pereira, Y. Berghoute, J. Douch, M. H. Mendonça and R. N. Singh, *Int. J. Electrochem. Sci.*, 4 (2009) 1074.
9. W. J. King, A. C. C. Tseung, *Electrochim. Acta*, 19 (1974) 493.
10. J. Haenen, W. Visscher, E. Barendrecht, *J. Electroan. Chem.*, 208 (1986) 273.
11. J. Haenen, W. Visscher, E. Barendrecht, *J. Electroan. Chem.*, 208 (1986) 297.
12. A. C. C. Tseung, S. Jasem, *Electrochim. Acta*, 22 (1977) 31.
13. S. Trasatti, G. Lodi in: S. Trasatti editor, *Electrodes of conductive mettalic oxides*, Part B. Elsevier, Amsterdam (1980), p. 521
14. S. Trasatti, *Electrochim. Acta*, 29 (1984)1503.
15. M. S. El-Deab, M. I. Awad, A. M. Mohammad, T. Ohsaka, *Electrochem. Commun.*, 9 (2007) 2082.
16. I. M. Sadiq, A. M. Mohammad, M. E. El-Shakre, M. S. El-Deab, *Int. J. of Hydrogen Energy*, 2011, DOI: 10.1016/j.ijhydene.2011.09.097, In Press.
17. R. N. Singh, J. P. Singh, A. Singh, *Int. J. Hydrogen Energy*, 33 (2008) 4260.
18. R. N. Singh, N. K. Singh, J. P. Singh, G. Balaji, N. S. Gajbhiye, *Int. J. Hydrogen Energy*, 31 (2006) 701.
19. M. E. G. Lyons, M. P. Brandon, *J. Electroan. Chem.*, 641 (2010) 119.
20. A. Salimi, R. Hallaj, S. Soltanian, H. Mamkhezri, *Anal. Chim. Acta*, 24 (2007) 594.
21. A. Salimi, H. Mamkhezri, R. Hallaj, S. Soltanian, *Sensor Actuat. B-Chem.*, 129 (2008) 246.
22. I. G. Casella, M. R. Guascito, *Electrochimica Acta* 1999, 45, 1113.
23. A.N. Frumkin, in: P. Delahay (Ed.), *Electrochem. and Electrochem. Eng.*, vol.3, Wiley Interscience, New York, 1963, p. 287.
24. S. Trasatti, O.A. Petrii, *Pure Appl. Chem.* 63 (1991) 711.
25. M. R. Gennero de Chialvo, A. C. Chialvo, *Electrochim. Acta*, 33(1988) 825.
26. R. N. Singh, N. K. Singh, J. P. Singh, *Electrochim. Acta*, 47 (2002) 3873.
27. M. Hamdani, M. I. S. Pereira, J. Douch, A. Ait Addi, Y. Berghoute, M. H. Mendonça, *Electrochim. Acta*, 49 (2004)1555.
28. B. Lal, M. K. Raghunandan, M. Gupta, R. N. Singh, *Int. J. Hydrogen Energy*, 30 (2005) 723.
29. M. Pourbaix, *Atlas of Electrochemical Equilibria in Aqueous Solutions*, NACE. Houston, Texas, 1974.
30. A. M. Mohammad, M. I. Awad, M. S. El-Deab, T. Okajima, T. Ohsaka, *Electrochim. Acta*, 53 (2008) 4351